https://doi.org/10.20965/jrm.2020.p0097

Paper:

Previous Announcement Method Using 3D CG Face Interface for Mobile Robot

Masahiko Mikawa*, Jiayi Lyu*, Makoto Fujisawa*, Wasuke Hiiragi, and Toyoyuki Ishibashi*****

*University of Tsukuba
1-2 Kasuga, Tsukuba, Ibaraki 305-8550, Japan
E-mail: mikawa@slis.tsukuba.ac.jp
**Chubu University
1200 Matsumoto-cho, Kasugai, Aichi 487-8501, Japan
***Gifu Women's University
80 Taromaru, Gifu, Gifu 501-2592, Japan
[Received August 3, 2019; accepted January 14, 2020]

When a robot works among people in a public space, its behavior can make some people feel uncomfortable. One of the reasons for this is that it is difficult for people to understand the robot's intended behavior based on its appearance. This paper presents a new intention expression method using a three dimensional computer graphics (3D CG) face model. The 3D CG face model is displayed on a flat panel screen and has two eyes and a head that can be rotated freely. When the mobile robot is about to change its traveling direction, the robot rotates its head and eyes in the direction it intends to go, so that an oncoming person can know the robot's intention from this previous announcement. Three main types of experiment were conducted, to confirm the validity and effectiveness of our proposed previous announcement method using the face interface. First, an appropriate timing for the previous announcement was determined from impression evaluations as a preliminary experiment. Secondly, differences between two experiments, in which a pedestrian and the robot passed each other in a corridor both with and without the previous announcement, were evaluated as main experiments of this study. Finally, differences between our proposed face interface and the conventional robot head were analyzed as a reference experiments. The experimental results confirmed the validity and effectiveness of the proposed method.

Keywords: passing each other, robot face, social human-robot interaction, gaze control, understandability

1. Introduction

Robots have been gradually entering our everyday lives in recent years. Although the designs of many industrial robots were utilitarian in the past, many sophisticated robots now work in public spaces, and there are many different types of robot, depending on their function. For example: a pet or rescue robot shaped like an animal [1–3], a vacuum cleaner robot with a round or polygon shape [4], a service robot whose upper body is humanoid [5–7], a social robot with a friendly design [8, 9], and an all-purpose humanoid robot [10, 11]. Many robots which interact with people have faces, and their faces serve important functions during these interactions.

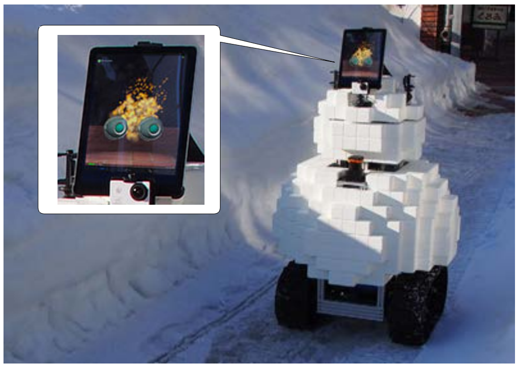

Fig. 1. Information service robot.

We are studying a teleoperational information service robot with a face in a shopping street environment, as shown in **Fig. 1**. When the robot wandered among pedestrians on a sidewalk, many children were happy to meet it. However, some adults seemed to feel uncomfortable and chose an alternative path to avoid the robot.

There are several problems to be solved for social robots including our service robot in a public space such as on a sidewalk. One of the problems is that it is difficult for people to understand the intentions of a robot from its appearance. For example, it is not clear for people in which direction the robot is going to go. In order for the robot to make a better impression on surrounding people, it is necessary for the robot to express its intentions more clearly.

In our previous study [12], we proposed a more natural intention expression method for a mobile robot. The robot had a dog-shaped head mounted on a pan-tilt unit. The robot rotated its head toward the direction where it

© Fuji Technology Press Ltd. Creative Commons CC BY-ND: This is an Open Access article distributed under the terms of the Creative Commons Attribution-NoDerivatives 4.0 International License (http://creativecommons.org/licenses/by-nd/4.0/).

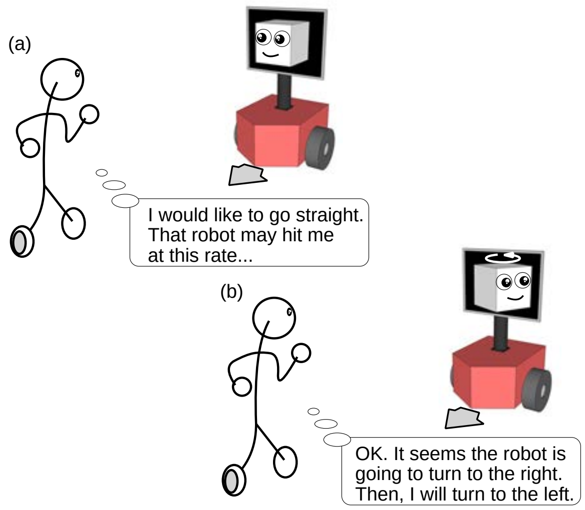

Fig. 2. Previous announcement using combination of face and gaze directions.

was going to go before starting to turn its body. Surrounding people could understand the traveling direction of the robot by this previous announcement from its head. However, the dog-shaped head had no other function but the previous announcement, and the moving parts might have a high cost and cause mechanical issues.

This paper presents a new intention expression method using a three dimensional computer graphics (3D CG) face model. We can design the CG model freely without considering the cost, and the panel screen can also have another function such as to provide information. The 3D CG face model is displayed on a flat panel screen, and the two eyes and the head can be rotated freely. When the mobile robot is about to change its traveling direction, the robot rotates its head and eyes toward the direction it intends to go, as a pedestrian shows their intended traveling direction by the direction in which they are gazing or facing. The angles of the eyes and the head and the traveling direction of the robot are calculated using the dynamic window approach (DWA) depending on the coordinates of a pedestrian, obstacles and a destination. As a result, an oncoming pedestrian can know the robot's intention to change its traveling direction in advance as shown in **Fig. 2**.

However, there is a phenomenon called "the Mona Lisa effect" where the gaze direction of the eyes of an artwork drawn on a 2D plane follows an observing person as she/he moves. Especially when a face drawn on a 2D plane is oriented straight-ahead and the gaze direction is also 0°, the Mona Lisa effect is especially observed [13]. However, an observer can perceive the gaze direction of a face image on a rotatable 3D head with eyes displayed on a flat panel display. The details are described in Section 2. Kawaguchi et al. investigated gaze direction estimation using a telepresence robot with a face display [14], and observed that it was possible to estimate the gaze direction. Its base was fixed on a table, and both the face display and a face image on the display could be rotated. Miyauchi et al. observed the effectiveness of eye contact between a person and a mobile robot using a rotatable 3D CG face displayed on the flat panel fixed on the robot's body [15]. Although the relevance of the perception of the eye contact, the robot's gaze direction and the robot's body behavior were discussed in detail, the robot only rotated on the spot without moving.

As can be seen from the related studies, a person can perceive approximate gaze direction from the rotatable 3D CG face and eyes. Therefore, in this study, we investigated to what extent an oncoming pedestrian can understand an intention of the moving robot performing the previous announcement. Concretely, experiments are conducted under a situation, where a research participant and the robot pass each other in a corridor. Although the situation is simple, since there is a set series of actions undertaken by the robot's face and body: an approach, the previous announcement, an avoidance, and a passing, it is necessary to evaluate the participant's understandability of the series of the actions. In addition, since one of the objectives in our project is to develop a robot that can make a better impression on a person as described previously, we also evaluated participant's impression of the robot's behaviors as a whole.

Three types of experiment were conducted to evaluate our proposed previous announcement method using the 3D CG face interface. First, as a preliminary experiment, an appropriate timing for the previous announcement was decided on, based on impression evaluations made by experimental participants. Secondly, as a main experiment, we evaluated the participant's understandability and impressions of the robot's behaviors when the participant and the robot passed each other in a corridor. Lastly, as a reference experiment, we analyzed the differences between our proposed face interface and the conventional dog-shaped head based on the participants' impressions.

2. Related Work

This section describes related work on two topics: behavior announcement methods and the Mona Lisa effect.

2.1. Announcement Methods

Some self-driving cars [a, b] use turn signals, brake lights, or reversing lamps in the same way as normal cars. A self-driving car developed by Jaguar Land Rover has large virtual eyes to interact with pedestrians, and makes eye contact to signal its intent [c]. Shindev et al. have proposed an intention expression method for a manipulator or a mobile robot using an arrow displayed by a laser projector [16]. The projected arrow shows the traveling direction of the robot. Matsumaru proposed a preliminary-announcement method for people around the mobile robot [17]. Four types of display methods using an omni-directional display, flat-panel display, laser pointer and projector were evaluated with or without displaying and vocalizing. Kanda proposed a service robot

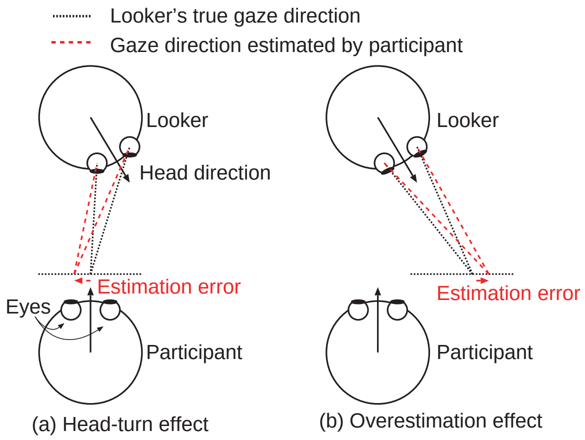

Fig. 3. Gaze direction estimation error.

for a shopping mall which has implemented several social behaviors [7].

2.2. Perception of Gaze Direction

Andrist et al. [18] and Admoni et al. [19] have discussed the importance of robot's gaze in human-robot interactions. There have already been many studies about human perception of gaze direction.

Gibson and Pick studied the perception of the gaze of another [20]. A human participant judged whether or not she/he was being looked at by a human looker. The looker sat opposite the participant. The looker turned her/him head to $0°$, $\pm 30°$ and looked in seven horizontal directions including the participant's front. The participants could perceive correctly that they were being looked at when the looker's head was front-facing. However, when the angle of the looker's head was $\pm 30°$, the gaze direction perceived by the participants had errors of $2.9°$.

Anstis et al. investigated perception of gaze direction in more detail using a picture of a looker's face on a television screen and a human looker [21]. They found that there were three effects that influenced an estimation of gaze direction: (a) the head-turn effect, (b) the overestimation effect, and (c) the TV-screen-turn effect. **Fig. 3** shows the head-turn effect and the overestimation effect. The head-turn effect describes how the participant perceives that the looker's gaze point is in the direction a little opposite to the looker's head direction, when the looker turns her/his head and faces the participant. The overestimation effect refers to the participant perceiving that the looker's gaze point is farther than the true gaze direction, even if the looker gazes exactly forwards as shown in **Fig. 3(b)**. The TV-screen-turn effect, whilst also describing how the participant can perceive the looker's gaze direction, has an estimation model that is different from those of the head-turn effect and the overestimation effect. However, "the TV-screen-turn effect probably arose because of the convex curvature of the TV screen."

Hecht et al. reported that the Mona Lisa effect broke down when the slant rotation angle of a picture of real face was greater than about $38°$ [22]. The direction of the face presented on a piece of cardboard was straight-ahead, and the gaze direction was also $0°$. This study showed that when a person looks a frontal face image presented on a flat panel, a strong Mona Lisa effect is observed.

On the other hand, when a person looks at a rotatable 3D face model with rotatable eyeballs displayed on a flat display, many studies suggest that she/he can perceive the gaze direction. Miyauchi et al. investigated the Mona Lisa effect for establishing eye contact [15]. The studies in [13, 23] investigated how cues relating to iris location and head orientation interact to estimate a perceived gaze direction. Moubayed et al. proposed a talking head using a 3D projection surface for limiting the Mona Lisa effect [24]. Gonzalez-Franco et al. proposed a single non-linear model for estimating gaze direction using stereoscopic images [25]. This mathematical model was designed in consideration of the head-turn effect and the overestimation effect. The image of the looker's face was displayed on a flat display, but since the stereoscopic images were used, the results of this study are in the same category as [20]. Kawaguchi et al. investigated a participant's estimate of a looker's gaze direction under several conditions [14]. The face image of the human looker was displayed on a rotatable flat panel display attached to a stand fixed on a table. When the fixed face image was displayed on the rotatable display, participants did not successfully estimate the looker's gaze direction, due to the Mona Lisa effect. On the other hand, the combinations of the rotated face and the fixed display or the rotated face and the rotated display worked well, as well as in face-to-face conditions. However, the overestimation effect was observed under some conditions.

From these studies, it can be concluded that a person can estimate a gaze direction of a looker, whose face is displayed on a flat display, by using rotatable face images. Although the overestimation or head-turn effects reduce the accuracy of the estimates of gaze direction, since a person perceives the angle of the gaze direction larger than the true value, these effects can be said to emphasize the gaze direction. Since it is important for the previous announcement to avoid eye contact between a pedestrian and the robot, and to inform her/him of the direction in which the robot is going, these effects are useful for the previous announcement.

3. System Configuration

Figures 4 and **5** show the teleoperated mobile robot system used in this study. An operator teleoperates a mobile robot using a gamepad and a keyboard. The robot is equipped with a laser range finder (LRF), and its position and orientation can be estimated by a simultaneous localization and mapping (SLAM) algorithm [d].

Since the purpose of this study is to evaluate the efficiency of our proposed face interface and its control method, the teleoperation and a task for the evaluations are simple. The task is for a pedestrian and the robot to pass each other in a corridor. The operator inputs destina-

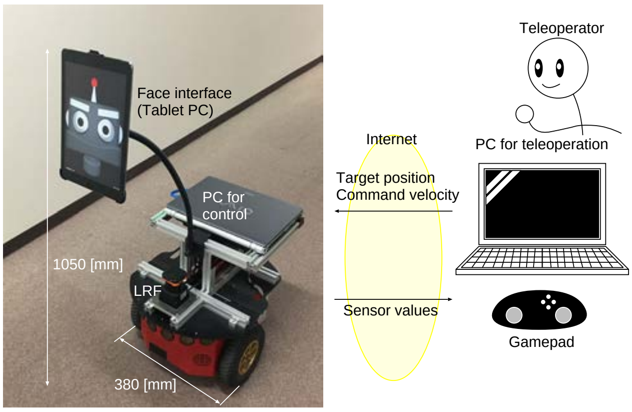

Fig. 4. Teleoperated mobile robot system.

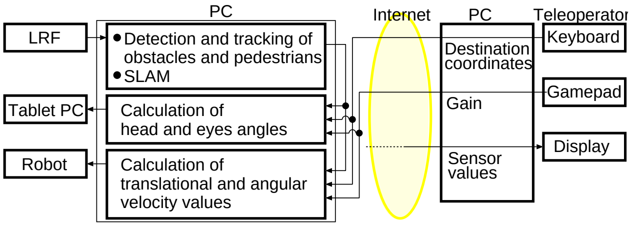

Fig. 5. Block diagram of teleoperation system.

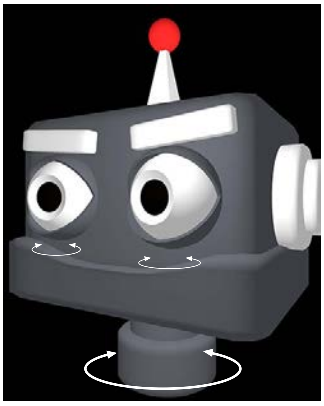

Fig. 6. Face interface made with 3D computer graphics.

tion coordinates using the keyboard once at the beginning of the experiment. The operator then adjusts the gains of the translational and angular velocity values of the mobile robot using the gamepad while the robot is traveling. The mobile robot is automatically controlled by the translational and angular velocity values calculated by our proposed method, as described later, when the robot and a pedestrian pass each other.

As shown in **Fig. 6**, the face is a 3D robot-like model made with CG. Although the tablet PC is fixed to the robot's body, the horizontal angle of the head and the two eyes of the 3D CG face model can be adjusted independently. Since the person's perception of gaze direction depends not only on the direction of the face but also the position of the irises within the robot's eyes [13], it appears that the goggle-eyed design helps the perception of gaze direction.

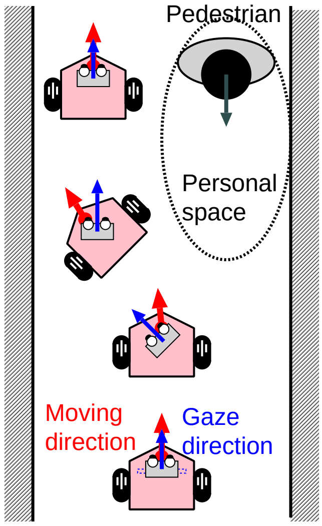

Fig. 7. Diagram to show the series actions of the robot's face and body when a pedestrian and the robot pass each other.

A particle-filter with a velocity-based motion model is used for detecting and tracking pedestrians [26]. The Inter Process Communication (IPC) library [e] is used for communication between the robot, the LRF and the PCs in this study.

4. Controls for Previous Announcement

The task of the mobile robot is to reach a goal position while avoiding pedestrians and obstacles. In particular, to inform the pedestrian of its traveling direction when they pass each other, motions of the head and the eyes are used, before beginning to change direction. Both a gaze control method and a motion control method for this previous announcement are described in this section.

4.1. Outline of Previous Announcement

Figure 7 shows a series of actions of the robot's face and body when the pedestrian and the robot pass each other in a corridor. First of all, when there is a sufficient distance between the robot and the pedestrian, the robot goes straight toward a goal position that the operator has previously inputted. Next, when the distance between the robot and the pedestrian is less than a threshold value, the robot decides which direction it should take depending on the relative position of the pedestrian compared to the robot. The face CG model shown in **Fig. 6** is rotated to the appropriate orientation to show her/him the robot's intended action, before changing the direction of the robot's body. At this time, the rotation angles of the head and the two eyeballs of the 3D CG face are controlled depending on the relative positions of the pedestrian, the robot and obstacles. The coordinates of these head and eyeball rotations help the pedestrian's perception of the robot's gaze

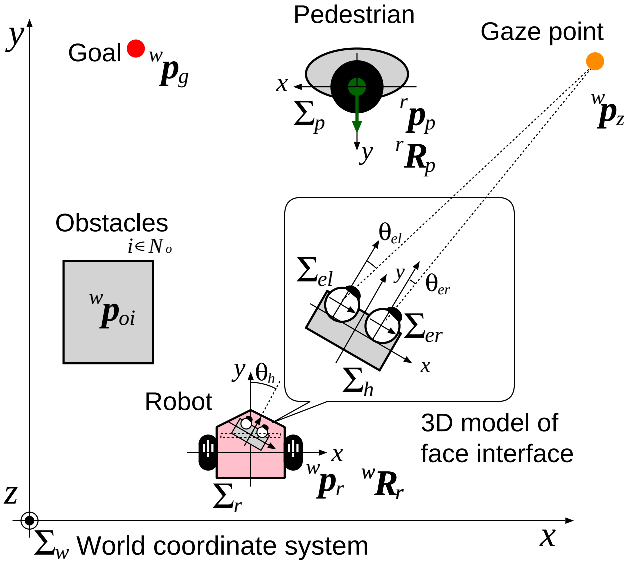

Fig. 8. Diagram to show the relations among the robot, the face interface, a pedestrian and obstacles.

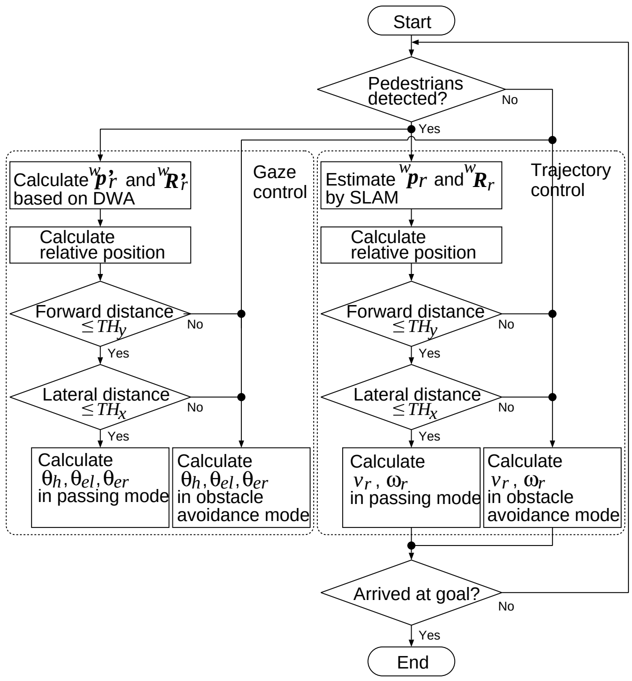

Fig. 9. Algorithm for trajectory and gaze controls.

direction. A short time later, the robot's body starts rotating to avoid the pedestrian. After passing each other, the robot goes straight toward the goal position.

In this paper, the DWA proposed by Fox et al. [27] is used for the trajectory control including obstacle avoidance, and the passing strategy proposed by Pacchierotti et al. [28] is used for the calculation of a pedestrian passing point. The previous announcement is realized by a combination of these two methods and our proposed face interface gaze control method. The details are described in the following subsections.

4.2. Coordinate Systems

Figure 8 shows the relationships between the mobile robot, the pedestrian, the goal position, obstacles, and each coordinate system. The origin of the mobile robot coordinate system Σ_r is at the rotational center between two wheels. The position ${}^w\boldsymbol{p}_r$ and orientation ${}^w\boldsymbol{R}_r$ of the robot in the world coordinate system Σ_w are estimated by the SLAM technique. Let an initial position and orientation of the SLAM map be Σ_w in this paper. The tablet PC is fixed to the robot's body, and the head and two eyes of the face 3D model displayed on the screen are rotated independently in a horizontal direction. Therefore, the robot head position ${}^r\boldsymbol{p}_h$ in Σ_r and the left and right eyes positions ${}^h\boldsymbol{p}_{el}$ and ${}^h\boldsymbol{p}_{er}$ in the head coordinate system Σ_h are constants, and the rotation matrices of the head and the left and right eyes are variables. ${}^r\boldsymbol{R}_h$ is calculated by the head angle θ_h, ${}^h\boldsymbol{R}_{el}$ and ${}^h\boldsymbol{R}_{er}$ are calculated by the left and right eyes' angles θ_{el} and θ_{er}, respectively, as shown in **Fig. 8**. Although the head reference coordinate system Σ_{h0} is not shown in **Fig. 8** for simplicity, let the origin of Σ_{h0} coincide with the origin of Σ_h, and the orientation of Σ_{h0} coincide with one of Σ_r.

The position ${}^r\boldsymbol{p}_p$ and the orientation ${}^r\boldsymbol{R}_p$ of the pedestrian in Σ_r are estimated by the pedestrian tracker. The goal position ${}^w\boldsymbol{p}_g$ in Σ_w is set manually by the teleoperator. The position ${}^w\boldsymbol{p}_{o_i}$ of an obstacle i ($i = 1 \sim \mathcal{N}_o$) in Σ_w is expressed as a part of a SLAM map. Since the pedestrian tracker does not discriminate between a moving obstacle and a pedestrian, the moving obstacle is recognized as the pedestrian in this paper. However, it is not difficult to discriminate between them by using another human detection algorithm, for example, the image based YOLO [29].

A gaze point ${}^r\boldsymbol{p}_z$ in Σ_r for the previous announcement is calculated based on a relation between the pedestrian and the mobile robot as described in Subsection 4.5.

Geometric relationships between these parameters can be expressed in every coordinate system. For example, the position ${}^w\boldsymbol{p}_p$ and the orientation ${}^w\boldsymbol{R}_p$ of the pedestrian in the world coordinate system Σ_w are calculated by the following equations by using the ${}^w\boldsymbol{p}_r$ and ${}^w\boldsymbol{R}_r$ values estimated by SLAM and the ${}^r\boldsymbol{p}_p$ and ${}^r\boldsymbol{R}_p$ values estimated by the pedestrian tracker.

$$ {}^w\boldsymbol{p}_p = {}^w\boldsymbol{p}_r + {}^w\boldsymbol{R}_r {}^r\boldsymbol{p}_p \quad (1) $$

$$ {}^w\boldsymbol{R}_p = {}^w\boldsymbol{R}_r {}^r\boldsymbol{R}_p \quad (2) $$

4.3. Pedestrian Passing Mode and Obstacle Avoidance Mode

Figure 9 shows the entire control system. When a pedestrian is detected by the pedestrian tracker and the robot is within a previously defined area surrounding her/him, the system enters into a pedestrian passing mode. Otherwise, it enters into an obstacle avoiding mode.

Figure 10 shows a time series of both gaze and robot motions based on a gaze control in the pedestrian passing mode. Let the x-axis of the world coordinate system Σ_w

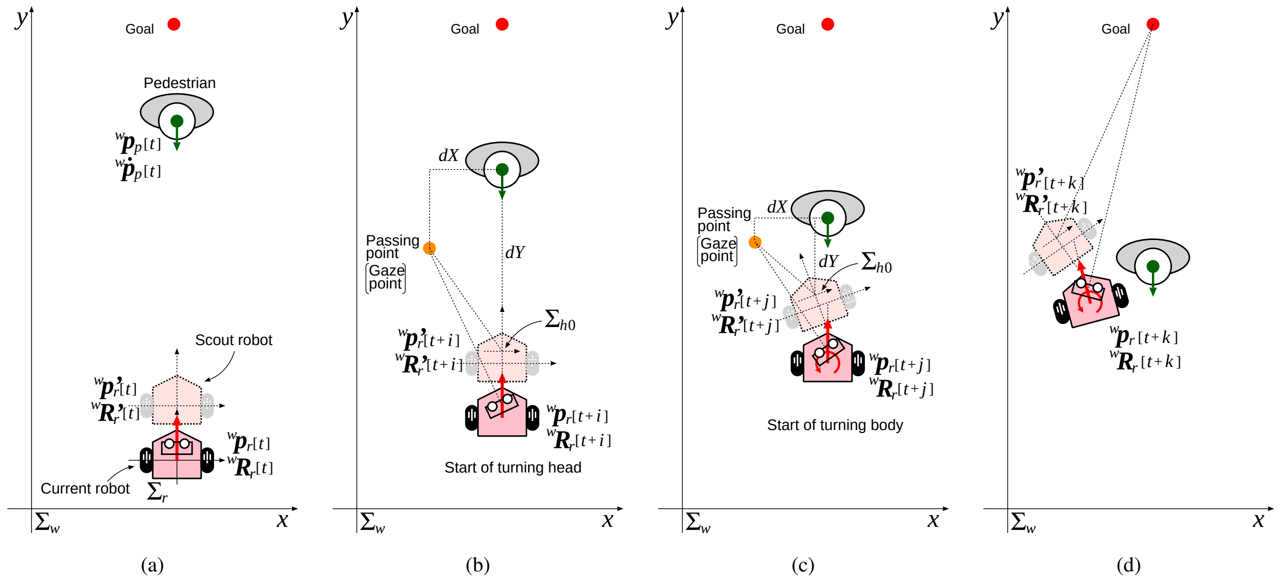

Fig. 10. Gaze control in pedestrian passing mode.

be in the direction across the corridor, and the y-axis of Σ_w be in the direction along the corridor. This mode mainly consists of the following four states.

(a) When the distance between the pedestrian and the robot is sufficiently large, the robot is guided toward the goal position by DWA. Let the current robot position at time t be ${}^w\boldsymbol{p}_p[t]$, and the orientation be ${}^w\boldsymbol{R}_r[t]$. Simultaneously, the estimated position ${}^w\boldsymbol{p}'_p[t]$ and orientation ${}^w\boldsymbol{R}'_r[t]$ after Δt_p [s] are estimated based on the current robot control inputs, the translational velocity v_r and the angular velocity ω_r, decided by DWA at the current position. This mobile robot at the estimated position is called the estimated robot in this paper.

(b) When the estimated robot fulfills the condition where a lateral distance $dX \leq TH_x$ and a forward distance $dY \leq TH_y$ between the pedestrian and the robot, a gaze point shown in **Fig. 10(b)** is decided by the method described in Subsection 4.5. The head angle θ_h, the left eye angle θ_{el} and the right eye angle θ_{er} are calculated based on the relations among the gaze point, the current position and orientation of the robot, and the head and both of the eyes are directed to the gaze point. This means that the robot can announce its traveling direction to the pedestrian by rotating its head and eyes before it actually begins to avoid the pedestrian.

(c) When the current robot has a lateral distance $dX \leq TH_x$ and a forward distance $dY \leq TH_y$ between the pedestrian and the robot as shown in **Fig. 10(c)**, the robot starts to avoid the pedestrian based on DWA. The calculation of ${}^w\boldsymbol{p}'_p[t]$ and ${}^w\boldsymbol{R}'_r[t]$ of the estimated robot is continued until the estimated robot passes the pedestrian.

(d) After the estimated robot has passed the pedestrian as shown in **Fig. 10(d)**, the goal position is set as the new gaze point. θ_h, θ_{el}, and θ_{er} are calculated based on this gaze point, and the head and the eyes are directed to the goal position as the previous announcement before the robot actually begins to move toward the goal position.

Figure 11 shows time series of both gaze and robot motions based on a gaze control in the obstacle avoidance mode. When no pedestrian is detected, the system is in the obstacle avoidance mode. Although there is no pedestrian near the robot, since some people further away from the robot may be observing it, the robot always executes the previous announcement behavior. The calculation of the estimated robot in this mode is the same as in the pedestrian passing mode. In this obstacle avoidance mode, we use a gaze point instead of the passing point. The gaze point is calculated in the following three steps: 1) ${}^w\boldsymbol{p}'_p[t]$ and ${}^w\boldsymbol{R}'_r[t]$ of the estimated robot are calculated in the same way with the passing mode. 2) The translational velocity v'_r and the angular velocity ω'_r for the estimated robot in ${}^w\boldsymbol{p}'_p[t]$ and ${}^w\boldsymbol{R}'_r[t]$ are calculated based on the DWA. 3) Let the gaze point be the position where the estimated robot moves at v'_r and ω'_r after Δt_g [s].

The head and the eyes are directed to the gaze point, as in the previous announcement, before the robot actually begins to avoid obstacles. Since the procedure in the obstacle avoidance mode is almost entirely similar to that in the pedestrian passing mode, we omit a detailed explanation here.

4.4. Trajectory Control

In this study, the computational method proposed by Pacchierotti et al. [28] was used for calculating the passing point shown in **Fig. 10**. In [28], a pedestrian and a

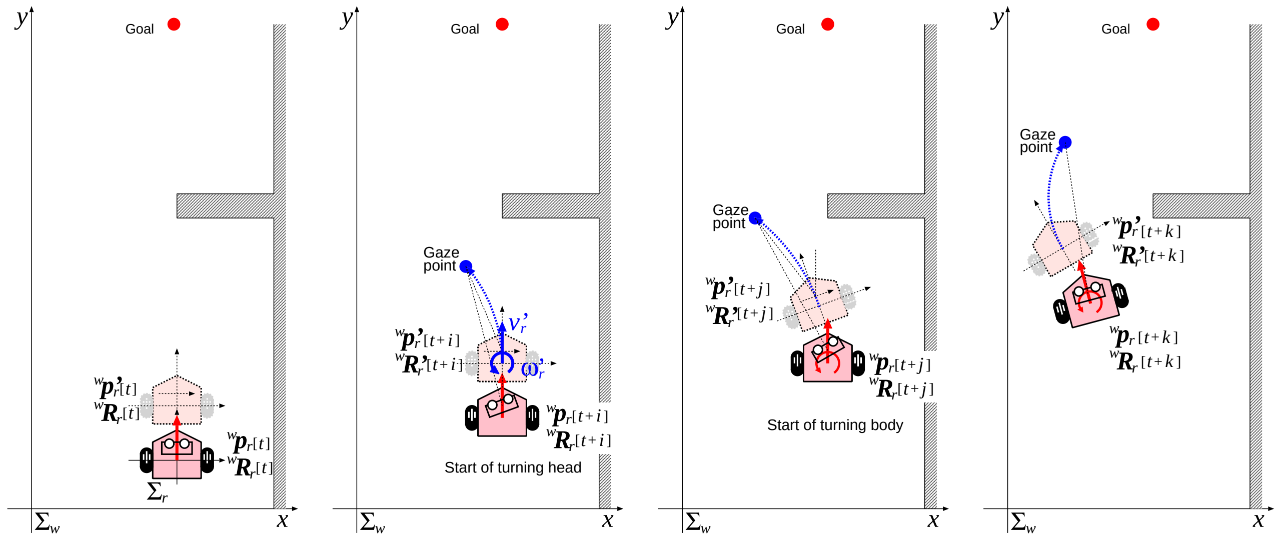

(a) (b) (c) (d)

Fig. 11. Gaze control in obstacle avoidance mode.

mobile robot can pass each other in a corridor with a comfortable lateral distance with consideration for personal space [30], and appropriate values of the distance are discussed. However, since the robot always turns right to avoid the pedestrian in the original method, we modify the method to make it possible for the robot to turn left or right.

Let the position of the pedestrian in Σ_w be ${}^w\boldsymbol{p}_p = ({}^w x_p \ {}^w y_p)^T$, the position of the mobile robot in Σ_w be ${}^w\boldsymbol{p}_r = ({}^w x_r \ {}^w y_r)^T$, and their velocities be ${}^w\dot{\boldsymbol{p}}_p = ({}^w\dot{x}_p \ {}^w\dot{y}_p)^T$ and ${}^w\dot{\boldsymbol{p}}_r = ({}^w\dot{x}_r \ {}^w\dot{y}_r)^T$, respectively. The passing point ${}^w\boldsymbol{p}_g = ({}^w x_g \ {}^w y_g)^T$ in Σ_w is calculated by the following equations in the same way as in our preliminary experiment [31].

$$ {}^w x_g = \begin{cases} {}^w x_p - (TH_x + 0.5 w_r) & \text{if} \quad {}^w x_r \le {}^w x_p \\ {}^w x_p + (TH_x + 0.5 w_r) & \text{otherwise} \end{cases} \tag{3} $$

$$ {}^w y_g = \frac{({}^w y_r - {}^w y_p)\,{}^w\dot{y}_r}{{}^w\dot{y}_r - {}^w\dot{y}_p} \tag{4} $$

Although the nearness diagram (ND) method [32] was used for the robot navigation in [28], the ND method is primarily designed for a holonomic mobile robot. Then we have chosen the DWA method suitable for a non-holonomic mobile robot. As shown in **Figs. 10(b)** and **(c)**, the robot is navigated to the passing point based on DWA with the current position of the robot, distance data from the LRF and the passing point, while the passing point is present between the pedestrian and the robot. When there is no passing point, the robot is navigated to the goal position using the current position of the robot, distance data from the LRF and the goal position.

4.5. Gaze Control for Face Interface

In order to notify surrounding people to the robot's intended traveling direction, the robot rotates its face and eyes to the passing point or the goal point. The computational method for the CG character's head and eye motions, proposed by Masuko et al. [33], is used for the gaze motions shown in **Figs. 10** and **11** in this study. Although the method in [33] determines the three types of angles: for the head, the eyes and the body of the CG character, since our CG face interface does not have a body, we modified some of the parameters in [33] to suit the shapes and the arrangements of the structural elements of our CG face interface.

As shown in **Fig. 8**, let the head angle relative to the head reference coordinate system Σ_{h0} be θ_h, and the left and right angles relative to the head coordinate system Σ_h be θ_{el} and θ_{er}, respectively. The passing point (= the gaze point) ${}^{h0}\boldsymbol{p}_g = ({}^{h0}x_g \ {}^{h0}y_g)$ is calculated using the following equations and the known parameters.

$$ {}^w\boldsymbol{p}_g = {}^w\boldsymbol{p}_r + {}^w\boldsymbol{R}_r \left({}^r\boldsymbol{p}_{h0} + {}^r\boldsymbol{R}_{h0}\,{}^r\boldsymbol{p}_g \right) \tag{5} $$

$$ \Leftrightarrow {}^r\boldsymbol{p}_g = {}^r\boldsymbol{R}_{h0}{}^T \left\{ {}^w\boldsymbol{R}_r{}^T \left({}^w\boldsymbol{p}_g - {}^w\boldsymbol{p}_r \right) - {}^r\boldsymbol{p}_{h0} \right\} \tag{6} $$

where, since Σ_{h0} is fixed on the robot's body, ${}^r\boldsymbol{p}_{h0}$ and ${}^r\boldsymbol{R}_{h0}$ are constant.

The angle of the line of sight relative to Σ_{h0}, ${}^{h0}\theta_g$ is calculated by the following equation:

$$ {}^{h0}\theta_g = \operatorname{atan2}\left({}^{h0}x_g, \ {}^{h0}y_g \right) \tag{7} $$

When the robot's face is turned to the gaze point, it is necessary to rotate the head and the two eyes naturally in the same way as a humans would. The sharing ratios of the head and eye angles proposed in [33] are used to calculate the angle of the head and the two eyes. Let the sharing ratio of the head angle be D_h, and the sharing ratio of the eye angle be D_e. The head angle θ_h and the left and right eye angles θ_{el}, θ_{er} are calculated as follows.

D_e and D_h are defined by the following equations.

$$D_e = \begin{cases} 1 & \text{if} \quad 0 \le \left|{}^{h0}\theta_g\right| < 15 \\ \dfrac{30 - \left|{}^{h0}\theta_g\right|}{15} & \text{if} \quad 15 \le \left|{}^{h0}\theta_g\right| < 30 \\ 0 & \text{otherwise} \end{cases} \quad \ldots \quad (8)$$

$$D_h = \begin{cases} 1 - D_e & \text{if} \quad 0 \le \left|{}^{h0}\theta_g\right| < 30 \\ 1 - \dfrac{\left|{}^{h0}\theta_g\right| - 50}{160} & \text{if} \quad 30 \le \left|{}^{h0}\theta_g\right| < 130 \\ 0 & \text{otherwise} \end{cases} \quad (9)$$

The head angle θ_h related to Σ_{h0} is calculated by the following equation.

$$\theta_h = D_h {}^{h0}\theta_g \quad \ldots \quad (10)$$

Next, the rotational matrix ${}^r\boldsymbol{R}_h$, the orientation of the head related to Σ_r, is calculated using θ_h shown in Eq. (10), and the gaze point ${}^h\boldsymbol{p}_g$ in the head coordinate system Σ_h is calculated using the following equation.

$${}^h\boldsymbol{p}_g = {}^h\boldsymbol{R}_r^T \left({}^r\boldsymbol{p}_g - {}^r\boldsymbol{p}_h\right) \quad \ldots \quad (11)$$

The positions of the gaze point in Σ_{el} and Σ_{er} are calculated by the following equations.

$${}^{el}\boldsymbol{p}_g = \left({}^{el}x_g,\ {}^{el}y_g\right)^T = {}^h\boldsymbol{R}_{el}^T \left({}^h\boldsymbol{p}_g - {}^h\boldsymbol{p}_{el}\right) \quad \ldots \quad (12)$$

$${}^{er}\boldsymbol{p}_g = \left({}^{er}x_g,\ {}^{er}y_g\right)^T = {}^h\boldsymbol{R}_{er}^T \left({}^h\boldsymbol{p}_g - {}^h\boldsymbol{p}_{er}\right) \quad \ldots \quad (13)$$

Thus, the angles of the left and right eyes are determined as follows.

$$\theta_{el} = \operatorname{atan2}\left({}^{el}x_g,\ {}^{el}y_g\right) \quad \ldots \quad (14)$$

$$\theta_{er} = \operatorname{atan2}\left({}^{er}x_g,\ {}^{er}y_g\right) \quad \ldots \quad (15)$$

4.6. Example of Previous Announcement Behavior

A simple example of the robot's behavior is discussed in this subsection. The robot started from the origin of Σ_w and moved in the y-axis positive direction. A pedestrian started from approximately the point $(0, 8000)$, and moved in the y-axis negative direction. Both of them passed each other at approximately the point $(0, 1700)$.

The trajectory of the robot and the gaze direction of the face interface are shown on the right in **Fig. 12**, and the trajectory and the traveling direction of the pedestrian are shown on the left in **Fig. 12**. The data was plotted at 0.5 s intervals.

It was observed that the robot could smoothly avoid a collision with the detected pedestrian, and the distance between the pedestrian and the robot when passing each other was about 600 mm. In addition, this figure also shows that the gaze direction of the robot was rotated appropriately to the traveling direction before the actual operation.

In this example, all the parameters for controlling the gaze direction and the mobile robot were the same as those in Section 5. When the pedestrian and the robot approach each other along the y-axis, since the gaze direction is about 40° at the beginning of the previous announcement, it appears to be easy for the pedestrian to understand the traveling direction of the robot. However, the longer the lateral distance dX between the pedestrian and the robot, the smaller the angle of the gaze direction. In this paper, when the the angle ${}^{h0}\theta_g$ of the gaze direction is less than 15°, the head is fixed and the only eyes are rotated based on Eqs. (8) and (9), and when ${}^{h0}\theta_g$ is more than 15°, both the head and the eyes are rotated. From previous studies, when ${}^{h0}\theta_g$ is less than about 5°–10°, the pedestrian may not be able to perceive the robot's gaze direction correctly. Because, according to [24] as described in Section 2, when the gaze direction of the front-facing CG face displayed on the flat panel display was from −7° to +5°, many participants perceived that they were being looked at by the CG face. According to [14], the gaze direction estimation models when the looker displayed on the flat panel display rotated only her/his eyes were shown as one of the experimental results, and even if the gaze direction is small, it seems that it can be estimated to some extent.

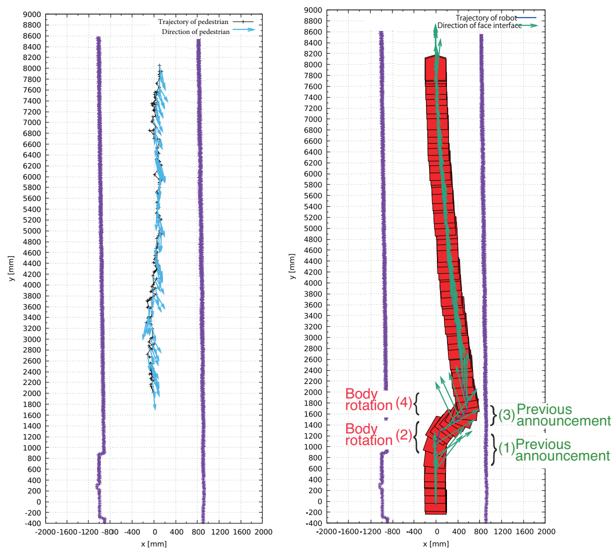

Fig. 12. Trajectories of the pedestrian and the robot with previous announcement.

5. Experimental Results

Three types of experiments were conducted to evaluate the effectiveness of the previous announcement method using the face interface. First, as a preliminary experiment, in order to decide appropriate timing for the previous announcement, different timings were evaluated. Second, in order to confirm the validity of the previous announcement, experiments both with and without the previous announcement were conducted, using the face interface on the flat panel display. Last, as a reference experiment, in order to confirm the validity of the face interface, experiments comparing the face interface and the

Table 1. Specifications of PC for controlling robot.

	PC
OS	Ubuntu 16.04 (64-bit)
CPU	Intel Core 2 Duo T9900
Memory	8 GB

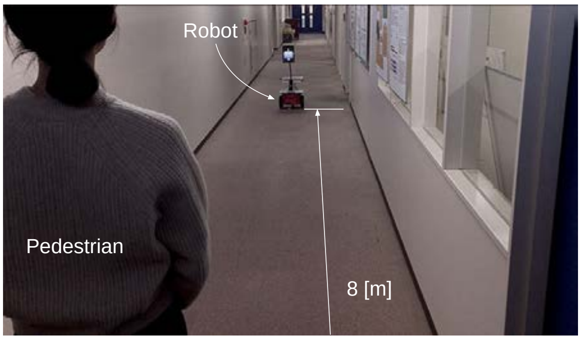

Fig. 13. Experimental environment.

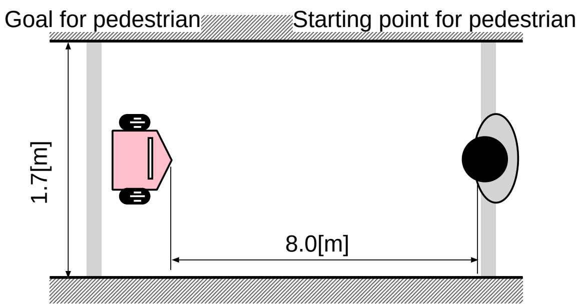

Fig. 14. Floor plan of the experimental environment.

conventional head used in our previous study [12] were conducted.

A total of 24 experimental participants in their twenties were recruited for the last three evaluation experiments. The group consisted of 10 females and 14 males participants, with an average age of 25.6 years. All of the participants were undergraduate or graduate students at the University of Tsukuba, Japan, and some were international students.

5.1. System Configuration

The system shown in **Fig. 4** was used in all of the experiments. However, since the teleoperation is not the main topic of this paper, the jobs of the operator were only to input a goal position and to monitor the robot status.

Table 1 shows the specifications of the PC mounted on the mobile robot.

5.2. Experimental Environment

The experimental environment is shown in **Figs. 13** and **14**.

Table 2 shows the parameters that were used in all of the experiments. We determined these values by referring to the values described in [28] and through preliminary experiments in this experimental environment. However, the translational velocity v_r of the robot is not a constant value but a variable. v_r is adjusted by the DWA method, and the average value of v_r was set to be about 0.30 m/s in this paper. Moreover, the actual control inputs v_a and ω_a for the robot are adjusted by the gain value, K ($= 0.0 \sim 1.0$) input from the gamepad, as shown in the following equations. K is used for the safe teleoperation.

Table 2. Experimental parameters.

Translational velocity of robot	0.30 m/s
Threshold of lateral distance TH_x	0.70 m
Threshold of forward distance TH_y	3.5 m

$$v_a = K v_r \quad (16)$$

$$\omega_a = K \omega_r \quad (17)$$

Since the experiments were conducted under safe conditions, $K = 1.0$ in all the experiments in this paper.

5.3. Experiment (1): Decision of Timing for Previous Announcement

The timing of the previous announcement is important for pedestrians. The previous announcement is executed Δt_p [s] before the robot begins to change its traveling direction. In order to determine the correct timing for the previous announcement, 24 participants evaluated four different timings for the previous announcement.

According to [34], an appropriate timing for the previous announcement was about 1 s. However, the timing might need to be varied depending on the experimental system. So, four different timing, $\Delta t_p = 0.5$, 1.0, 1.5, 2.0 s, were evaluated in this experiment, as a preliminary experiment for the following main experiment. When the participants evaluated these timings, they did not directly watch the behavior of the real robot but rather they watched prerecorded videos of the previous announcement behavior. This is because the robot's actual behavior is different depending on the pedestrian's behavior or position and the robot's movement or position for every experiment. Each participant could compare the different timings properly by watching the same videos. The parameters for the trajectory and gaze controls used are shown in **Table 2**, with the exception of the threshold of forward distance TH_y in the video. In this experiment, $TH_y = 3.6$ m. **Fig. 15** shows four types of video. Since the same parameters were used to control the robot in **Figs. 12** and **15**, it can be seen that the lateral distances between the robot and a pedestrian shown in both figures were approximately the same (about 600 mm). The participant watched the same video twice in a row, and the videos, each under the different conditions, were played in random order. After watching all the videos, they evaluated the adequacy of the four timings using a 5-point Likert-scale with values ranging from 1, bad, to 5,

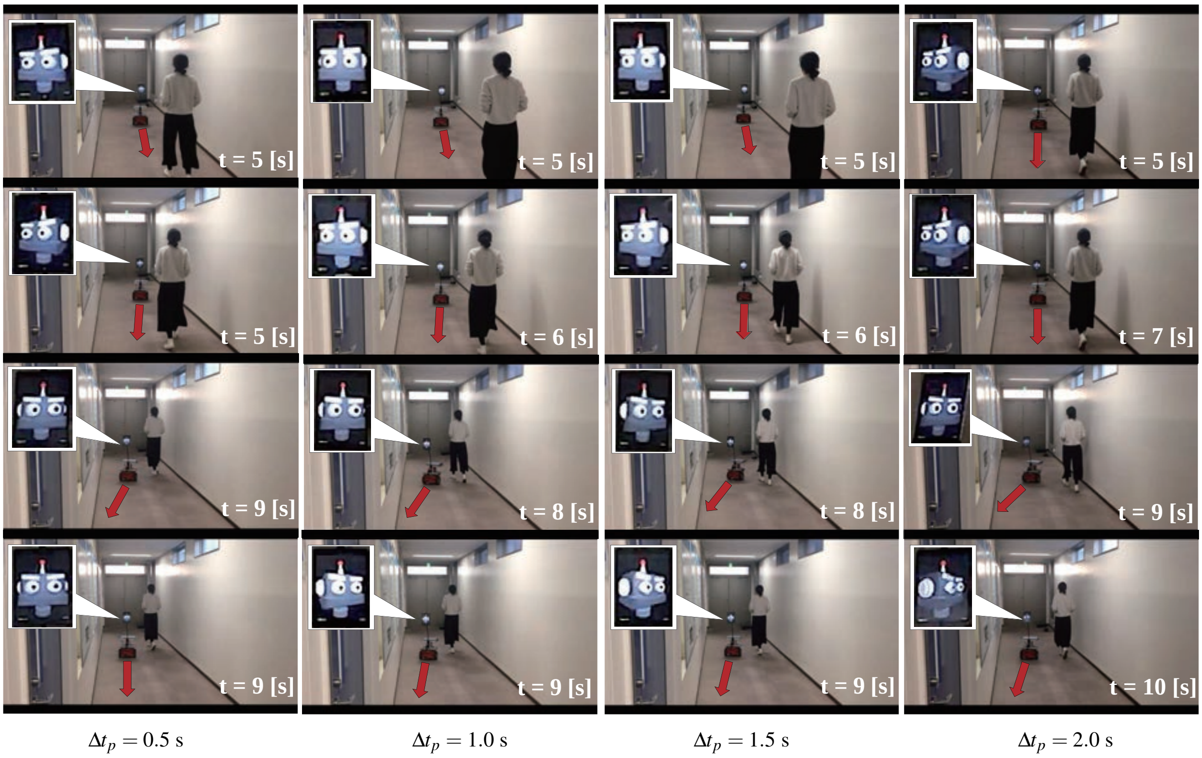

Fig. 15. Videos for timing evaluation.

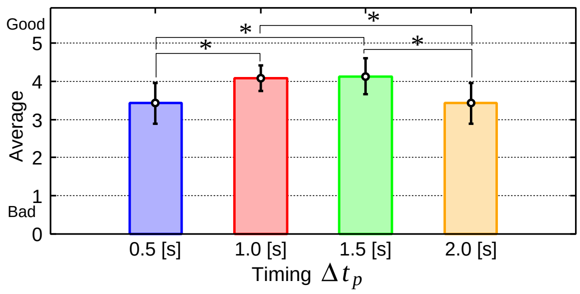

Fig. 16. Results from the evaluation of adequacy of timing.

good. The means and the standard deviations are shown in **Fig. 16**. **Table 3** shows the result of variance analysis. The F-value was $F = 4.24$ ($p < 0.01$(**)), and there was a significant difference between the different timings.

Next, Fisher's least significant difference (LSD) test was applied for multiple comparisons of the four timings, at a significance level of 5%. The results of the LSD test are shown in **Table 4**. There were significant differences between 0.5 and 1.0 s, 0.5 and 1.5 s, 1.0 and 2.0 s, and 1.5 and 2.0 s.

From these experimental results, the appropriate timing for the previous announcement appears to be between 1.0 and 1.5 s. We chose $\Delta t_p = 1.5$ s as the timing for the previous announcement in the following evaluation experiments.

However, this timing was chosen based on experiments conducted under limited conditions, where each participant watched each video only twice, and only one type of the mobile robot was used. The timing was decided on based on both the participants' first impressions and the suitability for the mobile robot used in this paper. Although the importance of the first impression was discussed in [35, 36], the number of our experiments might not be sufficient. It will be necessary to conduct a larger number of experiments under a greater range of conditions in future works.

5.4. Experiment (2): Comparison Between With/Without Previous Announcement

In order to confirm the validity of the previous announcement and the gaze control using the face interface, experiments to compare the situations with and without the previous announcement were conducted. Since the direction of the 3D CG face is set to straight-ahead when the previous announcement is not used, the face interface is always affected by the Mona Lisa effect. Under the experimental conditions with the previous announcement, the interface is affected only when the face turns to straight-ahead.

The number of the participants was also 24 in this experiment. Each participant and the robot passed each other twice in the corridor, as shown in **Figs. 13** and **14**. The head and the eyes of the face interface were rotated by our proposed previous announcement method in one of the two experiments. The components of the face interface were not rotated, and its eyes were kept looking straight ahead in the other of the two experiments. These two experiments were conducted in random order. Exam-

Table 3. Result of variance analysis for adequacy of previous announcement timing.

Evaluation item	Statistics	$\Delta t_p = 0.5$ s	$\Delta t_p = 1.0$ s	$\Delta t_p = 1.5$ s	$\Delta t_p = 2.0$ s
Adequacy	Mean	3.42	4.08	4.13	3.42
	Standard deviation	1.06	0.654	0.947	1.06
	Significance probability	$F = 4.24$ ($p < 0.01$(**))			

Table 4. Results of LSD test for multiple comparisons of the four timings.

	$\Delta t_p = 0.5$ s	$\Delta t_p = 1.0$ s	$\Delta t_p = 1.5$ s	$\Delta t_p = 2.0$ s
$\Delta t_p = 0.5$ s	–	0.016 ($p < 0.05$(*))	0.011 ($p < 0.05$(*))	1.0
$\Delta t_p = 1.0$ s	0.016 ($p < 0.05$(*))	–	0.88	0.16 ($p < 0.05$(*))
$\Delta t_p = 1.5$ s	0.011 ($p < 0.05$(*))	0.88	–	0.011 ($p < 0.05$(*))
$\Delta t_p = 2.0$ s	1.0	0.16 ($p < 0.05$(*))	0.011 ($p < 0.05$(*))	–

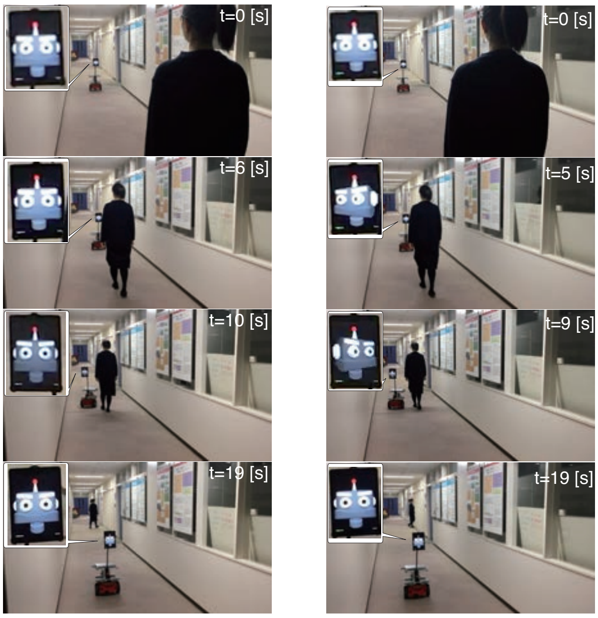

(a) Without previous announcement (b) With previous announcement

Fig. 17. Example of the passing-by experiment.

ples of the passing-by experiments under two sets of conditions are shown in **Fig. 17**. In the case without previous announcement, the CG face always looks in the same direction, regardless of the changing direction of the body. On the other hand, in the case with previous announcement, the CG face looks in different directions due to the change of the direction of the body.

After the two experiments, impression evaluations were conducted using two questionnaires, for investigating the participants' impression of the robot's behavior. First, each participant evaluated the understandability of the robot's behavior using a 5-point scale with values ranging from 1, confusing, to 5, obvious, as shown in **Table 5**. Next, each participant evaluated her/his impression using the Godspeed Questionnaire [37] shown in **Table 6**. Then, she/he answered the following question: "Please circle the number that the face was turned. 1. The first time, 2. the second time, 3. don't know." The results confirmed that all the participants had noticed the rotation of the 3D CG face.

Table 5. Questionnaire for understandability.

Scale	Item		
Understandability	Confusing	1 2 3 4 5	Obvious

Since the participant and the robot passed each other only once under each set of experimental conditions, a concern was that each participant would walk too freely along the corridor. Therefore, before conducting the experiments, the participants were asked to walk along the corridor as naturally and similarly as possible in both experiments. As a result, 23 out of a total of 24 participants passed the robot on its right side, and each participant passed on the same side in both experiments. Moreover, since the width of the corridor was about 1800 mm (it was about 4.7 times the width of the mobile robot), and it was not so wide for a person and the robot to pass each other, the differences in the trajectories between the two experiments were not large.

The means and the standard deviations of the evaluation results of the understandability are shown in **Fig. 18**, and the result of the t-test is shown in **Table 7**. The t-value was $t = -3.94$ ($p < 0.001$(****)), and there was a significant difference between the results with and without previous announcement. The mean value of the robot's behavior was better with the previous announcement compared to without announcement.

The means and the standard deviations of the impression evaluation results using the Godspeed Questionnaire are shown in **Fig. 19**, and the results of the t-test are shown in **Table 8**. Although there were some differences in the confidence intervals, there were significant differences in all the impressions.

These results show that our proposed previous announcement function works effectively. However, as described previously, each experimental participant walked

Table 6. The Godspeed Questionnaire.

Scale		Item		
Anthropomorphism	5	Fake	1 2 3 4 5	Natural
		Machinelike	1 2 3 4 5	Humanlike
		Unconscious	1 2 3 4 5	Conscious
		Artificial	1 2 3 4 5	Lifelike
		Moving rigidly	1 2 3 4 5	Moving elegant
Animacy	6	Dead	1 2 3 4 5	Alive
		Stagnant	1 2 3 4 5	Lively
		Mechanical	1 2 3 4 5	Organic
		Artificial	1 2 3 4 5	Lifelike
		Inert	1 2 3 4 5	Interactive
		Apathetic	1 2 3 4 5	Responsive
Likeability	5	Dislike	1 2 3 4 5	Like
		Unfriendly	1 2 3 4 5	Friendly
		Unkind	1 2 3 4 5	Kind
		Unpleasant	1 2 3 4 5	Pleasant
		Awful	1 2 3 4 5	Nice
Perceived intelligence	5	Incompetent	1 2 3 4 5	Competent
		Ignorant	1 2 3 4 5	Knowledgeable
		Irresponsible	1 2 3 4 5	Responsible
		Unintelligent	1 2 3 4 5	Intelligent
		Foolish	1 2 3 4 5	Sensible

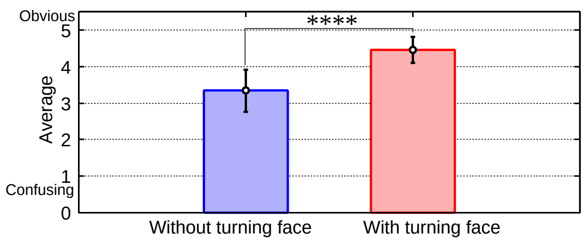

Fig. 18. Evaluation results for understandability.

along the corridor once under each set of experimental conditions. Moreover, since the width of the corridor was narrow, the robot's behaviors were almost the same. Hence, it is necessary to conduct further experiments under a greater range of conditions in future works.

5.5. Experiment (3): Comparison Between Proposed Face Interface and Conventional Head

Figure 20 shows two prerecorded videos. One was recorded during the experiment using the mobile robot with the dog-shaped head, and the other was recorded during the experiment using the robot with the face interface. 24 participants watched the same video twice in a row, and the videos, each under the different conditions, were played in random order. After watching all of the videos, they evaluated their impressions using two questionnaires, as in Section 5.4. First, each participant evaluated the understandability of the robot's behavior using the 5-point scale shown in **Table 5**. Next, each participant evaluated her/his impression using the Godspeed Questionnaire shown in **Table 6**.

The means and the standard deviations of the understandability evaluation results are shown in **Fig. 21**. The t-value was $t = -7.39$ ($p < 0.001$ (****)), there was a significant difference between the values for the dog head and the face interface. The mean value of the understandability for the face interface was better than for the dog head.

The means and the standard deviations of the results of the impression evaluation using the Godspeed Questionnaire are shown in **Fig. 22**. Although there were some differences in the confidence intervals, there were significant differences in all the impressions.

However, as can be seen in **Fig. 20**, the circumstances of the video recording varied between the two conditions. Although the differences between two conditions were confirmed, it cannot be said that the proposed CG face interface is better than the conventional dog head. It was not our original intention to prove that the face interface was better than the dog head, but rather we wanted to show that a pedestrian could understand the previous announcement using the face interface on the flat panel display. We believe that the face interface is at least as useful as the dog face without eyes.

5.6. Discussion

In order to confirm the validity of our proposed face interface, trajectory control method and gaze control

Table 7. Evaluation results of understandability.

Scale	Statistic	Without turning face	With turning face
Understadability	Mean	3.43	4.46
	Standard deviation	1.14	0.72
	Significance probability	$t = -3.94$ ($p < 0.001$(****))	

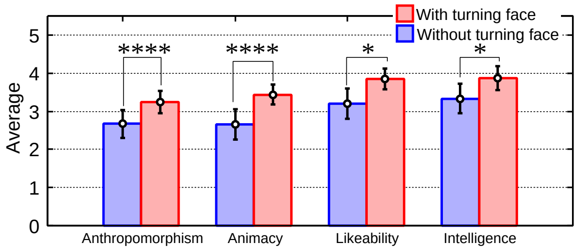

Fig. 19. Results of impression evaluation using Godspeed Questionnaire.

method, the comparison experiment was conducted under the following conditions. The first was conducted using the mobile robot with the 3D CG face interface with rotating head and eyes for the previous announcement. The second used the robot with the 3D CG face interface with fixed head and eyes. The results of the statistical analysis using data collected from 24 experimental participants confirmed the validity and the effectiveness of our proposed system.

Although some useful knowledge was obtained through the experiments in this paper, there are still many problems to be considered. First, although it was decided that the appropriate timing for the previous announcement was 1.5 s, since the translational velocity of the mobile robot and the parameters, TH_x and TH_y, that affect the timing were constant in this paper, it might be necessary to change the timing depending on a change in these constant values. Secondly, there was only one pedestrian and the robot in the corridor and the shape of the corridor was a rectangle, that is to say, the environment was too simple. Thirdly, the extent to which the overestimation effect or the head-turn effect affect the understandability and impression of a pedestrian in this study is unclear. It is necessary to conduct further basic experiments to study these effects. Since these effects emphasize the gaze direction, we hypothesize that these will have a positive effect on the previous announcement in the simple experimental environment used in this study. On the other hand, there may be both positive and negative effects in complex situations. An example of a negative effect could be that when there are two pedestrians and the robot, the previous announcement action that is easy to understand for one pedestrian may mislead the other.

Moreover, when two persons pass each other, the series of procedures are complex, such as a gaze direction control or an interpretation of a facial expression [38]. For example, it is stated in [39] that it is impolite to gaze at an unfamiliar person for a long time. This means that the behaviors exhibited before the previous announcement should be designed depending on the surrounding situation. In future work, it is necessary to conduct further experiments in a more realistic and complex environment such as a shopping street.

6. Conclusion

We proposed a new intention expression method using a three dimensional computer graphics (3D CG) face model. The 3D CG face model is displayed on a flat panel screen and the two eyes and the head can be rotated freely. The angles of the eyes and the head and the traveling direction of the robot are calculated using the DWA depending on the coordinates of a pedestrian, obstacles, and a destination. The mobile robot rotates the 3D CG face to the direction in which it is about to turn before starting to turn its body. Thus, this previous announcement allows an oncoming pedestrian to know the robot's intention. Three main types of experiment were conducted to confirm the validity and effectiveness of our proposed previous announcement method using the face interface. First, four different timing for the previous announcement were evaluated, and it was decided that the appropriate timing was 1.5 s. Second, differences between two experiments where a pedestrian and the robot passed each other in a corridor with and without the previous announcement were evaluated. Last, differences between our proposed face interface and the conventional robot head were analyzed. These experimental results revealed the validity and effectiveness of our proposed previous announcement method, gaze and trajectory control methods. However, since the experimental environments and conditions were too simple, it is necessary to conduct further experiments in a more realistic and complex environment such as a shopping street in future work.

Acknowledgements

This research was partially supported by JSPS KAKENHI Grant Number JP18K04041. We would like to express our gratitude to Research Professor Reid Simmons, the Robotics Institute, Carnegie Mellon University, USA, who offered us use of the IPC library [e] and the people tracking software using an LRF, that are used in the Roboceptionist system [40].

Table 8. Evaluation results using Godspeed Questionnaire.

Scale	Statistic	Without turning face	With turning face
Anthropomorphism	Mean	2.67	3.24
	Standard deviation	0.76	0.58
	Significance probability	$t = -2.94$ ($p < 0.001$(****))	
Animacy	Mean	2.65	3.42
	Standard deviation	0.80	0.52
	Significance probability	$t = -3.96$ ($p < 0.001$(****))	
Likeability	Mean	3.20	3.85
	Standard deviation	0.81	0.55
	Significance probability	$t = -2.25$ ($p < 0.05$(*))	
Perceived intelligence	Mean	3.33	3.89
	Standard deviation	0.77	0.63
	Significance probability	$t = -2.59$ ($p < 0.05$(*))	

(a) Conventional method (b) Proposed method

Fig. 20. Video images of previous announcement based on conventional and proposed methods.

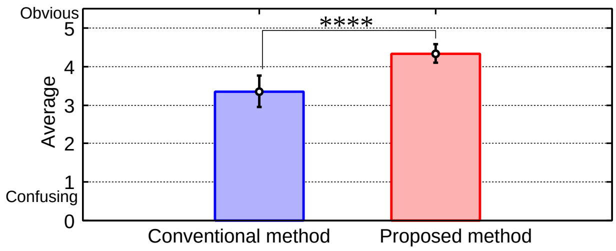

Fig. 21. Evaluation results for understandability.

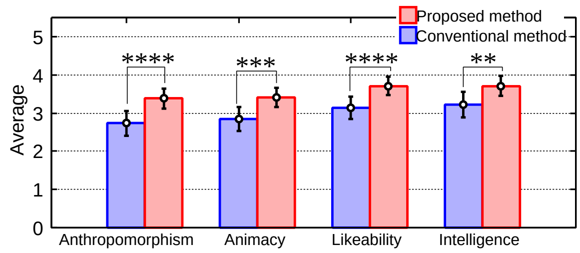

Fig. 22. Evaluation results using Godspeed Questionnaire.

References:

[1] T. Shibata, "Therapeutic seal robot as biofeedback medical device: Qualitative and quantitative evaluations of robot therapy in dementia care," Proc. of the IEEE, Vol.100, No.8, pp. 2527-2538, 2012.

[2] T. Shibata, "Aibo: Toward the era of digital creatures," The Int. J. of Robotics Research, Vol.20, No.10, pp. 781-794, 2001.

[3] D. Wooden, M. Malchano, K. Blankespoor, A. Howardy, A. A. Rizzi, and M. Raibert, "Autonomous navigation for BigDog," Proc. of 2010 IEEE Int. Conf. on Robotics and Automation, pp. 4736-4741, 2010.

[4] J. Jones, "Robots at the tipping point: the road to irobot roomba," IEEE Robotics Automation Magazine, Vol.13, No.1, pp. 76-78, 2006.

[5] S. Cremer, L. Mastromoro, and D. O. Popa, "On the performance of the baxter research robot," Proc. of 2016 IEEE Int. Symp. on Assembly and Manufacturing (ISAM 2016), pp. 106-111, 2016.

[6] A. K. Pandey and R. Gelin, "A mass-produced sociable humanoid robot: Pepper: The first machine of its kind," IEEE Robotics Automation Magazine, Vol.25, No.3, pp. 40-48, 2018.

[7] T. Kanda, "Enabling Harmonized Human-Robot Interaction in a Public Space," pp. 115-137, Springer Japan, 2017.

[8] E. Guizzo, "Cynthia Breazeal unveils Jibo, a social robot for the home," IEEE SPECTRUM, July 16, 2014.

[9] J. K. Westlund et al., "Tega: A social robot," Proc. of 2016 11th ACM/IEEE Int. Conf. on Human-Robot Interaction (HRI 2016), pp. 561-561, 2016.

[10] K. Kaneko, H. Kaminaga, T. Sakaguchi, S. Kajita, M. Morisawa, I. Kumagai, and F. Kanehiro, "Humanoid robot HRP-5P: An electrically actuated humanoid robot with high-power and wide-range joints," IEEE Robotics and Automation Letters, Vol.4, No.2, pp. 1431-1438, 2019.

[11] N. A. Radford et al., "Valkyrie: NASA's first bipedal humanoid robot," J. of Field Robotics, Vol.32, No.3, pp. 397-419, 2015.

[12] M. Mikawa, Y. Yoshikawa, and M. Fujisawa, "Expression of intention by rotational head movements for teleoperated mobile robot," Proc. of 2018 IEEE 15th Int. Workshop on Advanced Motion Control (AMC2018), pp. 249-254, 2018.

[13] D. Todorović, "Geometrical basis of perception of gaze direction," Vision Research, Vol.46, No.21, pp. 3549-3562, 2006.

[14] I. Kawaguchi, H. Kuzuoka, and Y. Suzuki, "Study on gaze direction perception of face image displayed on rotatable flat display," Proc. of the 33rd Annual ACM Conf. on Human Factors in Computing Systems (CHI'15), pp. 1729-1737, 2015.

[15] D. Miyauchi, A. Nakamura, and Y. Kuno, "Bidirectional eye contact for human-robot communication," IEICE – Trans. on Information and Systems, Vol.E88-D, No.11, pp. 2509-2516, 2005.

[16] I. Shindev, Y. Sun, M. Coovert, J. Pavlova, and T. Lee, "Exploration of intention expression for robots," Proc. of the 7th ACM/IEEE Int. Conf. on Human-Robot Interaction (HRI2012), pp. 247-248, 2012.

[17] T. Matsumaru, "Comparison of Displaying with Vocalizing on Preliminary-Announcement of Mobile Robot Upcoming Operation," C. Ciufudean and L. Garcia (Eds.), "Advances in Robotics – Modeling, Control and Applications," pp. 133-147, iConcept Press, 2013.

[18] S. Andrist, X. Z. Tan, M. Gleicher, and B. Mutlu, "Conversational gaze aversion for humanlike robots," Proc. of the 2014 ACM/IEEE Int. Conf. on Human-robot Interaction, pp. 25-32, 2014.

[19] H. Admoni and B. Scassellati, "Social eye gaze in human-robot interaction: A review," J. of Human-Robot Interaction, Vol.6, No.1, pp. 25-63, 2017.

[20] J. J. Gibson and A. D. Pick, "Perception of another person's looking behavior," The American J. of Psychology, Vol.76, No.3, pp. 386-394, 1963.

[21] S. M. Anstis, J. W. Mayhew, and T. Morley, "The perception of where a face or television 'portrait' is looking," The American J. of Psychology, Vol.82, No.4, pp. 474-489, 1969.

[22] H. Hecht, E. Boyarskaya, and A. Kitaoka, "The Mona Lisa effect: Testing the limits of perceptual robustness vis-à-vis slanted images," Psihologija, Vol.47, pp. 287-301, 2014.

[23] N. L. Kluttz, B. R. Mayes, R. W. West, and D. S. Kerby, "The effect of head turn on the perception of gaze," Vision Research, Vol.49, No.15, pp. 1979-1993, 2009.

[24] S. A. Moubayed, J. Edlund, and J. Beskow, "Taming Mona Lisa: Communicating gaze faithfully in 2d and 3d facial projections," ACM Trans. on Interactive Intelligent Systems (TiiS), Vol.1, No.2, pp. 11:1-11:25, 2012.

[25] M. Gonzalez-Franco and P. A. Chou, "Non-linear modeling of eye gaze perception as a function of gaze and head direction," Proc. of 2014 6th Int. Workshop on Quality of Multimedia Experience (QoMEX), pp. 275-280, 2014.

[26] J. Rollo, "Tracking for a roboceptionist," Master's thesis, School of Computer Science, Computer Science Department, Carnegie Mellon University, 2007.

[27] D. Fox, W. Burgardy, and S. Thrun, "The dynamic window approach to collision avoidance," IEEE Robotics Automation Magazine, Vol.4, No.1, pp. 23-33, 1997.

[28] E. Pacchierotti, H. I. Christensen, and P. Jensfelt, "Evaluation of passing distance for social robots," Proc. of the 15th IEEE Int. Symp. on Robot and Human Interactive Communication (RO-MAN 2006), pp. 315-320, 2006.

[29] J. Redmon and A. Farhadi, "YOLOv3: An incremental improvement," arXiv, abs/1804.02767, 2018.

[30] E. T. Hall, "The Hidden Dimension," Anchor Books, 1966.

[31] J. Lyu, M. Mikawa, M. Fujisawa, and W. Hiiragi, "Mobile robot with previous announcement of upcoming operation using face interface," Proc. of 2019 IEEE/SICE Int. Symp. on System Integration (SII2019), pp. 782-787, 2019.

[32] J. Minguez and L. Montano, "Nearness diagram (nd) navigation: collision avoidance in troublesome scenarios," IEEE Trans. on Robotics and Automation, Vol.20, No.1, pp. 45-59, 2004.

[33] S. Masuko and J. Hoshino, "Head-eye animation corresponding to a conversation for cg characters," Computer Graphics Forum, Vol.26, No.3, pp. 303-312, 2007.

[34] T. Matsumaru, S. Kudo, T. Kusada, K. Iwase, K. Akiyama, and T. Ito, "Simulation of preliminary-announcement and display of mobile robot's following action by lamp, party-blowouts, or beam-light," Proc. of IEEE/ASME Int. Conf. on Advanced Intelligent Mechatronics (AIM 2003), Vol.2, pp. 771-777, 2003.

[35] J. Xu and A. M. Howard, "The Impact of First Impressions on Human-Robot Trust During Problem-Solving Scenarios," Proc. of 2018 27th IEEE Int. Symp. on Robot and Human Interactive Communication (RO-MAN), pp. 435-441, 2018.

[36] K. Bergmann, F. Eyssel, and S. Kopp, "A Second Chance to Make a First Impression? How Appearance and Nonverbal Behavior Affect Perceived Warmth and Competence of Virtual Agents over Time," Proc. of Int. Conf. on Intelligent Virtual Agents, pp. 126-138, 2012.

[37] C. Bartneck, E. Croft, and D. Kulic, "Measurement instruments for the anthropomorphism, animacy, likeability, perceived intelligence, and perceived safety of robots," Int. J. of Social Robotics, Vol.1, No.1, pp. 71-81, 2009.

[38] E. Goffman, "Relations in public, Chapter The Individual as a Unit," pp. 3-27, Harper & Row, Publishers, Inc., 1971.

[39] E. Goffman, "Behavior in Public Places, Chapter Face Engagements," pp. 83-88, The Free Press Publishers, Inc., 1963.

[40] M. Makatchev and R. Simmons, "Incorporating a user model to improve detection of unhelpful robot answers," Proc. of Int. Symp. on Robot and Human Interactive Communication (RO-MAN 2009), pp. 973-978, 2009.

Supporting Online Materials:

[a] http://nutonomy.com [Accessed August 2, 2019]

[b] https://waymo.com [Accessed August 2, 2019]

[c] "Jaguar Land Rover's virtual eyes look at trust in self-driving cars," 2018. https://media.jaguarlandrover.com/en-gb/news/2018/08/jaguar-land-rovers-virtual-eyes-look-trust-self-driving-cars [Accessed August 2, 2019]

[d] Mobile Robot Programming Toolkit. http://www.mrpt.org [Accessed August 2, 2019]

[e] Reid Simmons. https://www.cs.cmu.edu/~ipc/ [Accessed August 2, 2019]

Name:
Masahiko Mikawa

Affiliation:
Faculty of Library, Information and Media Science, University of Tsukuba

Address:
1-2 Kasuga, Tsukuba, Ibaraki 305-8550, Japan

Brief Biographical History:

1994- NTT Access Network Systems Laboratories, Nippon Telegraph and Telephone Corporation
2001- NTT Service Integration Laboratories
2003- University of Tsukuba
2007- Visiting Researcher, The Robotics Institute, Carnegie Mellon University
2008- University of Tsukuba

Main Works:

- M. Mikawa, "Robust Wireless Communication for Small Exploration Rovers Equipped with Multiple Antennas by Estimating Attitudes of Rovers in Several Experimental Environments," J. Robot. Mechatron., Vol.29, No.5, pp. 864-876, 2017.
- M. Yoshikawa, M. Mikawa, and K. Tanaka, "A Myoelectric Interface for Robotic Hand Control Using Support Vector Machine," IEEE/RSJ Int. Conf. on Intelligent Robots and Systems (IROS2007), pp. 2723-2728, 2007.
- M. Mikawa and T. Tsujimura, "Sleep and Wake Control System Based On Mathematical AIM Model for Robot Vision System," Proc. of The Society of Instrument and Control Engineers (SICE) Annual Conf. 2005, pp. 2550-2555, 2005.

Membership in Academic Societies:

- The Institute of Electrical and Electronics Engineers (IEEE)
- The Robotics Society of Japan (RSJ)
- The Society of Instrument and Control Engineers (SICE)
- Japan Society for Fuzzy Theory and Intelligent Informatics (SOFT)

Name:
Jiayi Lyu

Affiliation:
Graduate School of Library, Information and Media Studies, University of Tsukuba

Address:
1-2 Kasuga, Tsukuba, Ibaraki 305-8550, Japan

Brief Biographical History:
2012- Beijing Language and Culture University
2017- Graduate School of Library, Information and Media Studies, University of Tsukuba
2019- Inner Mongolia Yili Industrial Group Co., Ltd.

Main Works:
- Human-robot interaction, market research, big data

Name:
Makoto Fujisawa

Affiliation:
Faculty of Library, Information and Media Science, University of Tsukuba

Address:
1-2 Kasuga, Tsukuba, Ibaraki 305-8550, Japan

Brief Biographical History:
2008 Received Ph.D. in Mechanical Engineering from Shizuoka University
2008-2010 Assistant Professor, Nara Institute of Science and Technology
2011- Assistant Professor, University of Tsukuba

Main Works:
- M. Fujisawa, T. Nakada, and M. Mikawa, "Particle-based Shallow Water Simulation with Splashes and Breaking Waves," J. of Information Processing, Vol.25, pp. 486-493, 2017.
- M. Fujisawa and K. T. Miura, "An Efficient Boundary Handling with a Modified Density Calculation for SPH," Computer Graphics Forum, Vol.34, No.7, pp. 155-162, 2015.
- M. Fujisawa, Y. Mandachi, and K. T. Miura, "Calculation of Velocity on an Implicit Surface by Curvature Invariance," J. of Information Processing, Vol.21, No.4, pp. 674-680, 2013.

Membership in Academic Societies:
- Association for Computing Machinery (ACM)
- The Institute of Electrical and Electronic Engineers (IEEE)
- Information Processing Society of Japan (IPSJ)
- The Institute of Image Electronics Engineers of Japan (IIEEJ)
- The Virtual Reality Society of Japan (VRSJ)

Name:
Wasuke Hiiragi

Affiliation:
Chubu University

Address:
1200 Matsumoto-cho, Kasugai, Aichi 487-8501, Japan

Brief Biographical History:
2010- Wakkanai Hokusei Gakuen University
2017- Chubu University

Main Works:
- Digital archive, meta data, local information resources

Membership in Academic Societies:
- Information Processing Society of Japan (IPSJ)
- The Japanese Society for Artificial Intelligence (JSAI)
- Japan Society for Digital Archive (JSDA)

Name:
Toyoyuki Ishibashi

Affiliation:
Gifu Women's University

Address:
80 Taromaru, Gifu, Gifu 501-2592, Japan

Brief Biographical History:
2016- Wakkanai Hokusei Gakuen University
2019- Assistant Professor, Gifu Women's University

Main Works:
- T. Ishibashi, W. Hiiragi, M. Mikawa, and T. Andoh, "Area specific metadata from local newspaper," J. of the Japan Society for Digital Archive, Vol.2, No.2, pp. 20-23, 2018.
- T. Ishibashi, W. Hiiragi, M. Mikawa, and T. Andoh, "Research of collecting lexicon for communication toward Regional comprehensive support service," J. of the Japan Society for Digital Archive, Vol.3, No.2, pp. 203-206, 2019.

Membership in Academic Societies:
- Japan Society for Digital Archive (JSDA)
- Japan Association for the Study of Learning Society
- Nippon Association for Librarianship (NAL)